How well can Regional Fluxes be Derived from Smaller-Scale estimates?

Kathleen E. Moore and David R. Fitzjarrald
Atmospheric Sciences Research Center
State University of New York at Albany
100 Fuller Rd.
Albany, N. Y. 12205

and

John A. Ritter
NASA Langley Research Center
Hampton, Va., 23665

NASA Research Cooperative Agreement
NCC1-135

Abstract

Regional surface fluxes are essential lower boundary conditions for large-scale numerical weather and climate models and are the elements of global budgets of important trace gases (Stewart, et al., 1989). Surface properties affecting the exchange of heat, moisture, momentum and trace gases vary with length scales from one meter to hundreds of kilometers. A classical difficulty is that fluxes have been measured directly only at points (towers) or along lines (from aircraft). The process of "scaling up" observations limited in space and/or time to represent larger areas has been done by assignings properties to surface classes and combining estimated or calculated fluxes using an area-weighted average. It is not clear that a simple area-weighted average is sufficient to produce the large scale from the small scale, chiefly due to the effect of internal boundary layers, nor is it known how important the uncertainty is to large-scale model outcomes. Simultaneous aircraft and tower data obtained in the relatively simple terrain of the western Alaska tundra were used to determine the extent to which surface type variation can be related to fluxes of heat, moisture and other properties. Surface type was classified as lake or land with aircraft-borne infrared thermometer, and flight-level heat and moisture fluxes were related to surface type. The magnitude and variety of sampling errors inherent in eddy correlation flux estimation place limits on how well any flux can be known even in simple geometries. Because of the presence of intrinsic and site-specific uncertainties, regional-scale flux of heat and moisture using aircraft observations in our study area can be reasonably verified to be estimated correctly from linear combinations of smaller-scale estimates to within a factor of 1.5. Flights at lower levels or in a more comprehensive or systematic pattern might be able to resolve the contributions from individual surface types better, but an experiment to test any scaling-up hypothesis is difficult to devise.

Introduction

Scaling up results from a local site to a region is the observationalists' counterpart to modelers' parameterization of the subgrid exchange. Every model of atmospheric dynamics, whatever its spatial domain or resolution, is dependent on assumptions or information about smaller-scale processes, particularly those processes involving exchange at the earth's surface. Current interest in global-scale models stimulates the demand for regional-scale estimates of surface fluxes, which are composed of fluxes from and to the variety of individual surface types comprising the surface mosaic in the region. The scale of "subgrid" variability can range from 10's of meters for the case of large eddy simulation models, to 10's of kilometers for global climate models. In many cases it is possible to make accurate measurements of the exchange with individual surface types using tower-based micrometeorological techniques, where surface homogeneity on a scale of 500m to 1 km or so is possible to attain. However, there are many questions about what the appropriate procedures are for making a regional-scale flux estimate out of estimates from smaller scales.

Various studies have approached the problem of how to deal with subgrid-scale variability. A desire to produce maps of roughness lengths led Mason (1988) and Vihma and Savijarvi (1991) to consider different methods of averaging z_0 or the drag coefficient, C_D, that would account for observed variability and preserve correct relationships among z_0, windspeed, and surface stress.

Large eddy simulation was used by Hechtel et al. (1990) to examine the effect of small-scale surface type variation on regional flux. The modelled inhomogeneous boundary had a negligible effect on the resultant flux profiles, compared to a homogeneous boundary with the same average properties. Surface radiative temperature was used as the determinant of the boundary condition.

One method for obtaining a regional-scale surface flux estimate is to use aircraft- based eddy-correlation measurements to obtain provide boundary-layer data over an entire region. An advantage to using aircraft is that choice of flight path permits budget studies that include estimates of advective terms (e.g., Lenshow et al., 1981, Ritter et al. 1990). The ABLE-3a experiment (Harriss, et al. 1992) is one of a series of experiments designed to obtain regional surface flux estimates of important trace gases using a combination of aircraft, tower-based, and chamber measurements. Each platform presents a flawed view of the regional flux. Aircraft estimates are only available when flying conditions are adequate, and factors such as clouds can interfere with some measurements. Flux estimates from towers can be made through the entire diurnal cycle for long periods of time (Fitzjarrald and Moore, in press), and are subject to fewer instrumental errors, but only a few surface types can be sampled adequately, as surface homogeneity (uniform fetch) on the scale of 500

m or so is a requirement for accurate estimates (Weill and Horst, in press). Chamber observations are important for understanding particular surface types responsible for trace gas emissions (Whiting et al ??), but, because they interfere with turbulence at the surface, they are not relevant to estimates of heat ,water vapor, and momentum fluxes considered here. We also do not consider large scale budgets based on horizontal mass convergence obtained from vertical profiles of winds and concentrations in radiosone networks (Yanai et al. 1973).

It is clear not only that sampling on a variety of scales is necessary to obtain a complete picture of regional trace gas, or other, exchange but also that some systematic procedure for compositing the data to the regional scale be employed. In recent model studies (Noilhan, et al., 1991), the adequacy of obtaining regional flux estimates from a mosaic of surface observations has been tested indirectly by comparing observations with regional model results, but it is not clear that the difference in properties of the surface types in the experimental area was large enough to affect heat and moisture flux estimates appreciably.

In this paper we examine some of these issues using observations from the ABLE-3b project, conducted in July and August of 1988 on and over the Yukon-Kuskokwim delta region of western Alaska. The region and details of the experimental design are discussed in Harriss et al. (1991). We concentrate on relating fluxes of heat and water vapor to the presence of lakes. The experimental area, a portion of which shown in Figure 1 is quite flat, with approximately 30% open water in the form of small shallow lakes. Though the area is highly heterogeneous at small scales, three simplified surface types have been identified as important to methane production: dry tundra, wet meadow, and open lakes. Bartlett et al. (in press) have shown from chamber measurements on small plots that the three surface types in western Alaskan tundra are quite different in their capacity to produce methane. Jacob et al (in press) and Ritter et al. (in press) found that there were differences in ozone uptake across the experimental area. We simplify the surface type classification further to include just two types: lake and land, for the decomposition of surface heat and moisture fluxes.

Regional-scale estimates demand some accounting of the surface heterogeneity. We believe that the ABLE-3a region should be as good a laboratory for testing the linear "scaling up" hypothesis for heat and moisture fluxes as can be found. We note that the surface patchiness is further complicated by the patchy distribution of clouds, which exert an influence on the surface heat and moisture fluxes by reducing the available solar input. In this paper we address the following questions:

1. How can the surface be characterized, using some remote sensing instrument such as the PRT-5 (radiometric temperature)(e.g., Hechtel, et al., 1990)? What characteristics does the surface have? Can this characterization be related to other remotely-sensed surface classifications?

2. Do the boundary layer characteristics (z_i , dz_i/dt, $d\theta/dt$) reflect the underlying surface inhomogeneity, or are they consistent with the smaller-scale measurements of surface heat flux?

3. At what height above the surface does the boundary layer cease to "feel" the variation in surface type?

4. Can we predict the flux from individual surface types? In particular, is the "linear scaling hypothesis", widely used by researchers (Bartlett,1990, Matson,1990) trying to scale up from chamber to regional scales, valid, i.e. is the regional flux simply the linear combination of the fluxes from individual surface types weighted by their fractional areal coverage?

Two aspects of surface classification are important when analyzing aircraft transects. First, one must identify the type of surface beneath the aircraft, and second, the geometry of the surface type variation must be taken into account in assessing the influence of the surface on the transport properties. The effects of very fine scale features will not be directly observable in the convective boundary layer. Thus we seek to identify the surface types and their shapes, and to relate a characteristic scale of the heterogeneity to the scale of the CBL thickness.

We first consider uncertainty attendant on aircraft flux estimates, and the limitations that such uncertainty places on our ability to scale up from tower to aircraft scales.

Procedures

The NASA Electra aircraft, used during the ABLE-3a mission, is equipped with a turbulent air motion measurement system (TAMMS) for acquiring data on the turbulent velocity components and temperature. Sensitive rotating balsa vanes in the TAMMS provide the data on the components of the wind; the motion of the aircraft is removed from these data through use of a high-resolution inertial navigation system. The resulting resolution in the vertical component of the wind is < 0.04 ms^{-1} . A Lyman-alpha hygrometer is used for fast humidity measurement, and a suite of other instruments can provide eddy estimates of CO, O_3, and CH_4 at a 20 Hz sampling rate . In addition, some variables such as the surface radiative temperature (sampled from a PRT-5) are sampled at a 5

Hz collection rate. Further details on the Electra instrumentation can be found in Ritter et al. (in press).

Simultaneous measurements of turbulent flux, radiative exchange, and mean quantities in the surface layer were made at site 30 km north of Bethel, AK (61^0 5.41' N, 162^0 0.92' W). The 12 m tower provided measurements of the surface sensible and latent heat flux, mean windspeed and direction, and air temperature and humidty. An A-frame structure nearby supported radiation instruments, including upward and downward looking short- and longwave radiometers (Fitzjarrald and Moore, in press).

We chose four flux flights in the Bethel area ,during which the aircraft was flown at a constant altitude for one to several hundreds of kilometers, for intensive study. Characteristics of the four days, based on the observations at the tower, are shown in Table 1. Two of the days were warm and sunny (days 210 and 215, flights 16 and 19, respectively), while the other two were overcast, with average surface heat flux less than 100 Wm^{-2} during the overflight periods. Soundings at the tower (Figure 2) site indicate that while on most days normal mixed layer development occurred, day 211 (flight 17) exhibited poor mixed layer development, while day 222 (flight 26) showed a typical mixed layer due in large part to mechanical mixing. Flight 26 represents a nearly-neutral stability case. Flight 16 was the only flight of the four in which the flight segments were stacked (Ritter, in press), such that a profile of the flux quanties could be constructed.

To examine the flux with surface type variation, each flight (or flight segment, in the case of flight 16) was broken into segments of 20 km. This length was chosen by examining plots of the variance of temperature or vertical velocity with segment length, and selecting the point where the change in the variances levels off.

Sources of uncertainty in flux estimates

Even after corrections for aircraft motion are made, the eddy correlation method of flux estimation imposes certain restrictions on the precision with which fluxes can be known (Wyngaard, 1983). On a tower, homogeneity and stationarity of the turbulence are prerequisites which suggest that the uniform fetch and sampling time must be adequate, in order to reduce the variance of the estimate. For aircraft measurements these requirements are met by ensuring that the flight segment is long enough--a criterion that varies with the substance whose flux is being measured, and the environment in which the measurement is made.

1. Ensemble-averaging: For an aircraft flux meaurement $\overline{w'c'}$ the relative error $\varepsilon_{wc} = [\ 2(r^{-}$ $^{2}+1)\lambda_{wc}]^{1/2}/\ L_{wc}$ where r_{wc} is the correlation coefficient between w and c, λ_{wc} is the integral scale of wc, and L_{wc} is the length of the flight segment (Lenschow and Stankov, 1986).
20 km segments yield errors of 33% of mean, in the best case (sensible heat). Much larger errors are probable when the correlation between w and c is lower.

Length scales increase with increasing height in the boundary layer, and the length scales for covariances vary according to the angle of the flight with respect to the wind

While these large relative uncertainties in the flux estimates are dismaying, we contend that the evidence we have points to an influence of the lakes on sensible heat flux. Figure (3) illustrates that the tower heat flux during flight 16 lies within the confidence bounds of the aircraft-extrapolated heat flux versus PRT-5 temperature. That is, the tower-based heat flux is higher in large part due to the higher surface temperature there; the tower is sampling only dry tundra, with no lake fraction in it.

2. Data treatment: where trends in the data exist, running mean removal , which effectively removes low-frequency contributions, can account for differences of 15%.

3. Instrumentation error: Ritter et al. (1990) have examined the effect of instrumentation error in the flux estimates made at single levels on the aircraft. They have found that instrumentation error constitutes 10-50% of the total error in flux estimation, depending on the total amount of flux. i.e. the larger percentage errors occur where the total flux was small.

4. Regression error: Where surface flux is estimated by extrapolation from a boundary-layer flux profile, as in flight 16, a least squares technique is usually applied to estimate the best fit through the data. Uncertainty in the estimates of regression coefficients yields standard errors of the surface flux quantities of about 10 %, for the best cases (heat flux). Trace gas fluxes show more variability, larger residuals from the regression, and therefore, much higher errors in the surface flux estimate.

5. Nonstationarity and other errors. As in any turbulent flux measurement, the underlying assumption is that the turbulence is stationary over the period of averaging.

Figure (4) from Flight 16 illustrates how these sources of error act to create uncertainty in the surface flux estimate for a single surface type. This figure also illustrates that an apparent discrepancy between the tower heat flux estimate and that from the aircraft can be explained by the combined effect of these errors. However, tower estimates of heat flux, particularly on sunny days, are usually higher than the extrapolated values from the aircraft flux profiles, because the tower is measuring fluxes only over land. Measurements of surface temperature at the tower are not always higher than all the 20 km flight segment estimates, as clouds can also influence the local surface temperature measurement. Figure (4) also demonstrates the inherent uncertainty in extrapolated surface fluxes for any particular surface type.

Estimates of the variation in net radiation over the region would aid in the interpretation of the flux estimates, as this quantity would place bounds on the sensible and latent heat fluxes, giving more confidence in these results. For the surface data, we find that the surface heat budget is in balance (Fitzjarrald and Moore in press), so that we doubt that our estimates of the sensible heat flux are biased by 20%.

A large possible source of error in scaling up to regional estimates of flux is the uncertainty atttached to the relative areas of each surface type known to contribute to the flux. Landsat and SPOT images have been used to make determinations of the extent of various soil and vegetation types, but these are subject to errors of their own. Consideration of the accuracy of chamber flux measurements, applied to these surface type classifications, is beyond the scope of this paper, but cannot be neglected in any final attempt to rectify measurements from different scales.

With these sources of error in mind, we proceed to probe for the answers to our initial questions.

Characteristics of surface

We chose to use the radiation temperature from the PRT-5 instrument for surface-type characterization. This instrument was sampled at a 5 hz rate, or 4 times more slowly than the turbulent variables (w', T',etc.). On a sunny day, PRT-5 temperatures exhibit a bimodal distribution, due to presence of small lakes. The land-water temperature difference is observed to be 12 K or more (Figure 5). For a given day, therefore, we determined a threshold temperature from examination of the radiation temperature time series below which a given observation was assigned to the category of "lake". Because on overcast days the dry land surface temperature does not rise

sharply ,variation tends to be smoothed out, and a sharp threshold between lake and land can not be detected. To include data from flights 17 and 26, therefore, we compare fluxes with the *average* surface temperature, reflecting the fact that on sunny days the lake fraction and the average T_0 are well-correlated. T_0, then, is representative of the surface classification as well as the surface forcing (due to the difference between T_0 and the air temperature).

The PRT-5 instrument has a 2 degree viewing angle, corresponding to a 40 m viewing length on the ground, if the airplane is at 1 km. This represents a much smaller land surface sampled than the flux footprint .Weill and Horst (1991) show that the flux footprint near the top of the boundary layer ($0.9z_i$) peaks at dimensionless downwind distance X=1, where $X=\frac{w*x}{Uh}$. If $w*$ is 2 ms^{-1}, U is 5 ms^{-1}, and h is 1000m, then the flux footprint extends 2.5 km from the point of measurement. At the lowest measurement level flown by the aircraft (0.1 h) the footprint extends only 0.5 km upwind. The footprint is measuring the downwind region of influence of a particular surface point, on the flux at some height. Depending on the flight track relative to the wind, surface radiation temperature and the flux may not correlate on a small scale at all. Over a 20 km flight segment, however, we are characterizing an average property of the surface, which should not be that different if displaced 2.5 km to either side. In along-wind or against-wind flight tracks it might be possible to conduct a lagged correlation to show an association of the flux with specific surface features. Weill and Horst also recognize that an important aspect of the flux footprint problem is actually the inverse of the estimate provided here, i.e., that of discovering the surface source distribution from the measured flux.

An ordinary runs test can be used to detect clumped distributions of dichotomous data in transects (Gibbons, 1985). For an ordered sequence of two types of observations (e.g., lake and land) the expected value (E) for the number of runs or sequences (U) of either type, in a random distribution is:

$$E(U)=1 + 2m\,(N-m)/N$$

where m is the total number of lake points and N is the total number of observations in the transect. Clustered data exhibit a lower number of runs than the expected number. The standardized U is :

$$Z_U = [\,U + 0.5 - E(U)]\,/s_u$$

where s_U is the standard deviation of U: $s_U= (2m(N-m)[2m(N-m)-N] / [N^2 - (N-1))^{1/2}$. The statistic Z_U is a large negative number if clustering is exhibited in the data.When this test is applied to the radiation temperature data from the aircraft, highly significant negative values of this statistic result, indicating a clumped distribution along the transect.. Therefore, spatial distribution of low-

temperature points is not random; rather it is patchy, confirming the notion that the PRT-5 is really detecting a feature such as lakes interspersed with dry land.

Histograms of surface temperatures and the lake "sizes" (based on number of consecutive data points below the threshold temperature) observed in the aircraft transects from Flight 16 are shown in Figure (6). The lake size distribution is dominated by a large number of single- or few-point observations of low radiation temperature. These single-point observations could be the result of flying over very small lakes, or streams, or over the edge of lake, highlighting the limitations inherent in trying to depict two-dimensional features from transects. Total water fraction varies among 20 km flight segments from 13% to 58% of the observations. Where correlations of fluxes or other quantities with water fraction have been done, the criterion for "lake" points was set at 15 or more consecutive observations classified as "lake", i.e., only lakes greater than 300 m in length along the surface temperature transect were included.

The effect of transect sampling a spatial array of circular "lakes" was tested by randomly locating circles in an x,y array with radii generated randomly from a Gaussian distribution. Transects were then "flown" over the array. These tests indicate that distribution of lake sizes is similar to that obtained from the radiation temperature, i.e. small sizes dominate the distribution, due to the low probability of a transect corresponding exactly to the circle diameter. Therefore, the mean lake size obtained from transects is smaller than the actual mean.

Transects were also made over a digitized surface classification map derived from Landsat photos (U.S. Department of the Interior, Fish and Wildlife Service) of the region between 61 and 62 degrees N latitude, and -163 and -165 W longitude. The tower area is in the extreme southwest corner of this map, and the map includes 2 flight legs from Flight 26, and one from Flight 17. We obtained a color photograph of this image and digitized it with 80 m resolution and 16 gray scales. Lakes were easily identifiable and the image was simplfied to describe only the lake-land difference (Figure 1). The total water area in the digitized photo region was 15%. Time series of surface radiation temperatures from the aircraft, when compared to co-navigated transects on the photo indicated some rough correspondence, but also substantial divergence between the two "views" of the surface. Some of this divergence is probably due to navigational error in the transects over the photo. The East-West flight leg of flight 26 yielded a zonal gradient in surface temperatures, with the colder areas in the west. This gradient is also observable in the total water area, and total lake perimeter derived from the photo (Figure 7). Thus on a relatively large scale (over 1 or more degrees of longitude) there is agreement between the PRT-5 temperature classification and the Landsat image.

Clearly the height and degree of influence of surface type variation on boundary layer properties depends on the size of the inhomogeneity, e.g. it is possible to imagine a situation where the lake area is distributed among many very small lakes which would not have the same influence on the boundary layer as fewer, large lakes. In part this stems from the fact that internal boundary layers develop at the upwind edge of surface type discontinuities; such IBLs do not contribute to the flux in a fashion which is representative of the surface beneath them. If the lakes tend to be large, however, the area covered by IBLs would be small relative to the lake, and the effect of the IBLs would be small. For this reason it is important to obtain some measure of the scale of the inhomogeneity.

One measure of a length scale for surface type variation is the integral scale of the PRT-5 temperature autocorrelation, determined from the lag at which the autocorrelation becomes zero. For several of the flight legs this distance was about 1000 m. The length scale is observed to vary along a flight leg, reflecting the fact that lake size and number vary through the region. The length scale is partly a function of lake size, and partly of distance between lakes. While the average lake size is comparable to the integral scale of $w\theta$, the characteristic $\lambda_{PRT\text{-}5}$ is comparable to, or larger than z_i. Integral length scales computed from the autocorrelation functions for the heat flux, and for w' and T' are about 500m or less,at the lowest flight levels, increasing at higher heights.

A related, but slightly different scale is obtained from the semivariogram (Matheron, 1963). This geostatistic is computed as : $G(l)= (1/2*N)*\Sigma\ ((x(i) -x\ (i+l))^2$

where N is the number of points in the series, x(i) is the value of the variable whose semivariogram will be plotted, l is the spatial lag between two points. The point at which a plot of semivariance against separation (l) levels off is known as the range. During flights 16 and 19 the surface radiation temperature and the slow air temperature sensor gave a range of about 1 km, while the vertical velocity and fast temperature each had a range of 500 m.

Yet another approach to the question of how large the scale of the surface inhomogeneity has to be, in order to be detected by aircraft flux measurement, is to calculate the characteristic time scales for the flow across the lakes. Such a scale could be compared to the boundary-layer convective mixing time scale, $z_i/w* = 10\text{-}15$ minutes. A typical surface windspeed of 3-4 m/s and a typical lake diamter of 500 m would yield a trajectory of perhaps 100s at the longest, much shorter than the

mixing time scale. Hechtel et al. (1990) point out that this is why the thermals in their LES are not "attached" to surface features, but are advected from their source relatively quickly.

Lastly, some guidance may be gained from modelling studies seeking to find the optimal means of averaging surface roughness over inhomogeneous terrain (e.g. Mason, 1988). Here a "blending height" is defined very roughly as $l_b = L_c/200$, where L_c is a periodic length scale for the change in surface roughness. Above this height, changes in surface roughness are found to have little impact on the momentum transport or the velocity profile. If we take L_c to be the 1 km length scale of the lake-land contrast, then the 150m flight level of the Electra is well above the blending height. On the other hand, if the gradient in surface temperatures observed in flight 26 is related to a surface roughness change (for example, with changing vegetation type), then the characteristic length scale is some tens of kilometers, and the flight level is well within the region of surface influence.

To summarize these explorations of the surface type description: it is important to derive some measure of the characteristic size and geometry of inhomogeneity, for example, lake diameter and shape. These can be integrated into a single statistic, such as the ratio of the area to the perimeter of the lakes, which might be characteristic of the region. Any characteristic length scale of inhomogeneity should be compared to the boundary layer depth, z_i; , and to the height at which the measurement is made, z.

Boundary-Layer Characteristics

Sequences of boundary layer balloon profiles taken at the tower site (Fitzjarrald and Moore, in press) indicate that on most days a normal mixed layer develops such as that expected over homogeneous terrain, conforming qualitatively to the slab or jump model for mixed layer development. To examine the question of whether the mean properties of the boundary layer reflect the local surface fluxes at the tower (assumed to include only land-based flux) or the regional fluxes (some mixture of lake and land), a simple jump model for boundary layer growth was constructed (Tennekes, 1973). The model used the actual surface sensible heat flux observed at the tower as the forcing for the boundary layer growth, and comparisons with the balloon soundings done at the tower site were made. Modelled boundary layer growth rates (dz_i/dt) were on the order of 100m/hour during the time of most rapid growth in late morning and early afternoon on sunny days (local solar noon at the tower was 1400). This result is comparable to those observed in the soundings , although the model growth rates are higher earlier in the morning and lower in late morning, due to the fact that the model is not calculating the "filling in" of the morning temperature

inversion. The ultimate height of the mixed layer was slightly less in the model than those obtained from the soundings (Figure 8); however, within the error due to estimation of z_i ,and uncertainty about subsidence rates and entrainment fluxes, the actual height of the mixed layer and its rate of growth and warming are consistent with the tower-based heat flux estimates.

Cross-sections of the boundary layer are provided by the DIAL LIDAR aerosol backscattering photos from the NASA Electra This system and example images are presented in Browell et al. (in press). During flight 26, the boundary layer depth varies over several hundred meters, being smallest 1150m in the wetter areas nearer the coast (where the heat flux observed by the aircraft is smallest) and highest 1500m in the upland areas surveyed by the north-northwest leg of the flight. Figure (8) indicates the range of mixed layer depths observed by the DIAL aerosol instrument during flight 26. This range of z_i would correspond to a 30% difference in surface heat flux integrated over the day, based on the results of the model, suggesting a corresponding difference of 40-50% in the underlying lake fraction. The DIAL results are consistent with the observed differences in heat flux during Flight 26, and with the modelled response of the boundary layer to the actual surface forcing. Several of the aerosol backscatter photos depict a definite slope to the mixed layer top, as well as to the overlying cloud deck. The aerosol backscatter was also much greater in the western reaches of the flight, near the coast, possibly due to the advection of marine aerosol in that region.

Thus, while the boundary layer in the region of the tower (an upland tundra area with numerous small lakes) appears to be mainly influenced by the land surface heat flux, the larger regional boundary layer does respond to variation in the underlying surface type. This result is consistent with the notion that the length scale of the inhomogeneity relative to the boundary layer depth, l/z_i, is a relevant statistic for determining the influence of surface type variation.

Flux estimates

Flight 16--

Flight 16 covered a more limited area than the other flights being considered here, each of which included the wetter coastal areas where the lakes were somewhat larger. Nontheless, there is still substantial variation in surface type represented. Of the flights under consideration here, only flight 16 consisted of a "stacked" pattern of flight segments, such that flux profiles could be constructed. Thus we discuss the results of this flight separately from the other flights. Where flight

segments are stacked in this way, the flux at the surface can be obtained by extrapolation from the least-squares fit to the flux profile.

Extrapolated sensible heat flux during flight 16 and radiation surface temperatures are correlated. The 12 m tower-based heat fluxes are consistently higher than the extrapolated values; however, the radiative temperature measured at the ground site was also higher than that recorded by the PRT-5 (Figure 1). The tower heat flux on this graph is within the confidence bounds of the regression. Thus, at least some of the difference between the aircraft measurements and the ground site measurements can be accounted for by the surface types being sampled by each method. Surface moisture fluxes obtained by extrapolation do not bear any relationship to the mean PRT-5 temperature measurement. The tower-based moisture flux measurement is within the range of the extrapolated values. The trace gases (CH_4, CO, etc.) do not exhibit a clear dependence of extrapolated flux on surface type classified by radiation temperature for this flight.

At the lowest flight level in flight 16 there is a negative correlation between water fraction and heat flux, but this correlation is non-existent at the middle and upper flight levels, suggesting that the boundary layer no longer feels the surface type variation at 400 m. The ratio l/z_i is fairly small (0.3) in this flight, as the lakes were small and the boundary layer well-developed. In all likelihood this is because thermals merge together, becoming most defined in the middle region of the boundary layer, and are not attached to any surface feature. The boundary layer depth was not observed to vary along a flight track during this flight.

Flights 17, 19, 26--

A budget equation for any scalar, C, in the boundary layer (ignoring advection) can be written:

$$dC / dt = - \delta (w'C') / \delta z$$

where w'C' is the turbulent flux of C. If the boundary layer has reached a steady state with respect to the scalar C, then the flux profile is non-divergent. Using an integrated form of the above equation, and ignoring the role of the entrainment flux in determining the distribution of C, it is apparent that the surface flux is then predicted by the flux at a given flight level , z. The flux "surveys" at 150m flight level in flights 17,19, and 26 are taken to represent the surface fluxes.

For modeling purposes it is often convenient to use simple parameterizations of the surface fluxes, for example, for heat:

$$F = - U * C_H * \Delta \Theta$$

where $\Delta\Theta$ is the difference between the potential temperature of the air and the surface temperature, and C_H is a bulk transfer coefficient which varies with stability and with the surface type. Using the single-level aircraft measurements of heat flux as representative of the underlying surface flux, C_H can be calculated utilizing the PRT-5 as the surface temperature measurement. Flight 19 yields values of 5.4×10^{-3} and 7.5×10^{-4} for land segments and ocean segments, respectively, illustrating the difference in stability between these two environments. Over the warmer inland surfaces during flight 26, C_H was 1.1×10^{-3}, while on the other overcast day, during flight 17, C_H was 1.96×10^{-3}.

The drag coefficient (bulk transfer coefficient for momentum) presents a more complicated situation, as calculated momentum flux at flight level is not always negative(a consequence of the larger uncertainty in momentum flux estimation). Flight 26 offers the most consistent picture because of the higher wind-speeds at flight level and the more nearly neutral conditions. Here the drag coefficient is 1.83×10^{-3} over the cooler coastal areas, and 2.93×10^{-3} inland. Because of the nearly neutral stability prevailing during this flight, the drag coefficient variation is not attributable to variation in stability; rather, it is likely that different roughnesses, perhaps due to different vegetation types, is being reflected in C_D.

When all the flights are combined there is a positive correlation between mean PRT-5 temperature(our measure of surface type) and heat flux in the low-level flight legs. In contrast to the results from the extrapolated profiles, moisture flux is also correlated with surface temperature, when all flights are combined (Figure 9). Because the surface-air temperature difference is the driving force for surface heat flux, we also present similar relationships for heat and moisture fluxes with temperature difference (Figure 10), with the expectation that this would be a more general expression of the relationship of flux to surface type. The most general expression would include the surface windspeed, as in the parameterization above; plots with $U\Delta T$ have greater unexplained variance, possibly because boundary-layer winds don't accurately reflect surface-layer winds. The most dramatic effects of surface type are seen in the contrast between fluxes observed over the ocean and those over land (flights 17, 19), in which the fluxes are zero or negative over the ocean and immediately rise as the aircraft crosses the coast line. The relationships of heat flux with lake fraction, where those could be determined, indicate that the land flux (zero lake fraction, i.e. the intercept) is 0.05 to 0.09 $ms^{-1}K$ (60 to 108 Wm^{-2}), depending on the day, while the lake heat flux is not significantly different from zero. The small lake heat flux obtained in this manner is consistent with observed air-surface temperature differences of zero, or slightly positive values.

If the "linear hypothesis" is true, then an expression for the surface flux, estimated from the aircraft flight level, would be:

$$F = \sigma F_L + (1 - \sigma) F_T$$

where F is the flux, σ is lake fraction and the subscripts L and T refer to lake and tundra, respectively. Using the bulk tranfer relation for heat flux given above, and assuming there is a difference in the bulk transfer coefficients over lake and tundra, we have:

$$F = - U * (\sigma C_L + (1 - \sigma) C_T) * (\sigma \Theta_{0L} + (1 - \sigma) \Theta_{0T} - \Theta_{AIR})$$

This simple model can be used to test the validity of the linear hypothesis, at least for heat flux. Figure (10) includes the curve obtained for values of C_L=2 e -3 and C_T = 4 e-3. The windspeed used in the figure was 2 ms^{-1}. When the observations are regressed against the model results, the resulting R^2 is 0.83 and the slope of the line is 0.95.

On day 222 (flight 26), the soundings at the tower site indicate the presence of a cloud layer extending from 3100 to 4000 m at 1000 LT, lowering to 2250m by 1600 LT. The cloud layer was responsible for the low overall surface fluxes on this day, and for the poor distinction between lake and land radiation temperature observations (i.e. the lack of a bimodal distribution in PRT-5 temperatures). Aircraft DIAL measurements of aerosol scattering also detect this cloud layer, which slopes down to 1500-2200 m near the coast. The height and thickness of this denser aerosol layer in the eastern reaches of flight 26, near the tower, correspond to the cloud layer measured there by the balloon soundings. The mixed layer depth, well below the cloud layer, also slopes upward toward the inland locations, being shallowest near the coast. An area of increased aerosol scattering within the mixed layer existed in the westernmost areas, near the coast, probably reflecting the advection of marine aerosol inland. The inland locations, particularly the eastern leg of the flight 26 pattern, shows the highest sensible heat flux, the highest PRT-5 temperature values, the warmest boundary layer temperatures, and the deepest mixed layer -- a set of conditions indicative of normal mixed layer behavior. The difference in z_i between the coastal areas and the center of the pattern, nearest the tower, was about 300m, as noted previously. This variation in z_i along the flight track on this day indicates that the influence of surface type variation extends through the mixed layer, by determining the development of the mixed layer in time.

During flight 26 ozone flux was greater (more negative values) where the surface radiation temperature was lower (the wetter,coastal areas). This has been reported by Ritter et al.(in press) and Jacob, et al. (in press). Ozone flux during this flight was also correlated with the momentum flux, a

fact we note is true for the surface layer as well. In addition, there is a greater flux of methane from these wetter, coastal areas. These areas are also a greater source of moisture than the inland areas sampled by flight 26, resulting in a trend with mean surface temperature which is opposite that for flights 17 and 19. The underlying cause of these trends is the fact that horizontal windspeed as twice as high near the coast as it was inland during this flight. While the momentum flux is stronger near the coast, the drag coefficient is lower, as indicated above. There is a strong negative correlation during this flight between PRT-5 temperature and the windspeed. We find that our PRT-5 classification is consistent with the qualitative classification discussed by Ritter et al., which was based on satellite images of the area.

Discussion and Conclusions

We have found that the radiative surface temperature as measured by the PRT-5 can be used for surface classification in the ideal test case of western Alaska tundra, where variation in elevation is not a complicating factor, and where the dominant surface type variation is due to the presence of numerous small lakes. This tool would be more useful had more complete measurements of the radiative fluxes are made. For example, Luvall and Holbo (1991) have made measurements in several environments of the surface temperature from airborne thermal scanners. They have found that different surface types can be accurately determined from their thermal response to the net radiation, i.e. they define a "thermal response number" , $TRN=[\Sigma R_N \Delta t]/\Delta T$, where the numerator represents the total net radiation received in a time interval Δt, and ΔT is the difference in radiative temperature observed over the time interval. In their studies, aircraft-borne measurements are made in successive passes about 30 minutes apart.

It has been proposed or assumed by several authors (e.g. Avissar and Verstraete, 1990) that for exchanges which are surface-type dependent, the large scale flux is an average of the fluxes from the various types, weighted by the relative area in the the region:

$$F= (\Sigma A F)/ \Sigma A$$

In this scheme, features such as lakes are lumped together, regardless of size, and their contribution to the flux assumed to be based on their total area. As pointed out above,the relative importance of internal boundary layers varies with the size of the inhomogeneity; this is one reason that the linear hypothesis might fail. The hypothesis itself is rarely, if ever tested.

For scalar fluxes such as heat and moisture it is possible to relate boundary-layer fluxes, observed by an aircraft, to surface features. Our results suggest that the linear scaling-up hypothesis

may be valid for heat flux in Western Alaska (with fairly large scale inhomogeneities) and possibly for moisture flux, but we are unable to validate it for the trace gases examined in ABLE-3B, due to the relatively larger uncertainties in the flux estimates and the fact that the simple lake-land classification may not be adequate. For heat flux, there may be substantial uncertainties in flux estimates obtained by extrapolating to the ground. Some of the apparent discrepancies between regional-scale fluxes observed by aircraft and those measured on the ground can be attributed to the differences in surface type being sampled by each technique.

An important problem in large-scale models has been the choice of technique for averaging subgrid variation in z_0 or other roughness parameter, so as to obtain realistic estimates of the surface stress. A variety of analytical methods were tested against a model of boundary-layer flow, by Vihma and Svijarvi (1991). Similar results were obtained by the model and from the drag-coefficient averaging scheme developed by Mason (1988). Where the surface was determined to have just two roughness categories (water and forest), the effective z_0 was shown to vary non-linearly with the percentage land surface and to be higher than a simple area-weighted average of the two $\ln(z_0)$. More importantly for the context of this paper, it was shown that for a given fraction of land surface, effective z_0 was affected by the length scale of the homogeneous fetch, i.e. internal boundary layers increased the roughness parameter when the fetch values were very low. Estimates of z_0 for the areas covered by the flights in this study are difficult to reconcile with the suface observations at the tower. Flight 26 is the only flight where most of the momentum flux estimates are negative; the nearly neutral conditions on that day indicate that changes in the drag coefficient estimated at 150m are due to roughness differences. Flight-level C_D estimates are comparable to those obtained at the tower, with the result that the z_0 observed at flight level are implausibly high (1.3 cm for water, and 4.49m for land) , compared to the tower-based estimate of 0.5 cm (Fitzjarrald and Moore, in press). Surface roughness may be a particularly difficult parameter to scale up, from tower to aircraft.

A recent study (Said and Druilhet, 1991) approached the question of how to account for surface inhomogeneity in large scale models utitlizing aircraft flux data over the ocean at 50m. They averaged estimates of the bulk transfer coefficients for momentum, heat and moisture from small to large scales, concluding that, despite the large variability in estimates of transfer coefficients, the average of the local results was consistent with an aereal average. In effect, this interpretation would be a validation of the linear hypothesis.

Linear combinations of local estimates of transfer were used by Wetzel and Chang (1988) to determine regional evapotranspiration in a numerical model, taking account of subgrid-scale variation in surface type. They approached the problem of surface heterogeneity by utilizing the nonlinear

relationship between soil moisture and evaporation for each subgrid estimate. They point out that evapotranspiration is a highly nonlinear function of several variables, including soil water availability, vegetation characteristics, and others, highlighting the desirability of accounting for subgrid-scale variation.

The length scales, geometry, and amplitude of surface inhomogeneities are important to their possible effect on boundary-layer properties. Austin et al. (1987) have attempted to distinguish varying surface sink strengths for CO_2 (varying biomass productivity) on the basis of aircraft measurements in combination with Landsat images of the wind-damaged areas. They found that a surface-type homogeneity of 3 km was required, to detect with certainty the surface type variation. Another numerical model (Hechtel, et al. 1990) incorporating large-eddy simulation, indicated that surface patchiness was not detectable in the boundary layer properties, presumably because mixing is very efficient throughout the boundary layer. The surface in that study, however did not have exhibit surface inhomogenieties of the areal size or amplitude of the lake-land contrast in western Alaska, and fluctuations in surface temperature did not appear to be strongly associated with surface features to the extent that they were in this study.

Given the inherent errors in flux estimates, it may only be possible to decompose regional flux into fluxes from component surface types very broadly. This fact places a strong limitation on how well we can know the ways future changes in the surface will influence exchange properties (e.g. permafrost melting, tropical deforestation (Dickinson and Henderson-Sellers, 1988)). It also means that subgrid parameterization for large scale models will remain uncertain.

Future experiments to make measurements of regional-scale fluxes should make use of satellite-based surface classifications, in the design phase of of the experiment. A hierarchy of sampling methods continues to be desirable to provide both ground truth for aircraft-based estimates and tests for alternative methods of reconciling measurements made on different scales. The "blending" of flux-carrying eddies from different surface types must be dependent on the ratio of the length scale of the inhomogeneity to the boundary layer scale; fractionally, the boundary layer scale doesn't change very much, so that the scale of inhomogeneity should determine the experimental approach to a scaling-up experiment. Low-flying aircraft appear be able to distinguish among different surface types (Desjardin et al.,), but this advantage comes at a cost of limiting the region that can be sampled. Ultimately, though, an experiment to test the validity of any particular scaling-up hypothesis may not be feasible.

Page Intentionally Left Blank

Table 1. Average surface conditions during aircraft overflights, determined at the tower site . Day is Julian day, and T_{bb} (K) is the surface temperature from a downward-looking infra-red radiometer with emissivity assumed =1.0. Average air temperature is θ_{AIR} (K) , R_N is net radiation, H is surface sensible heat flux (Wm^{-2}), and U is windspeed at 12 m (ms^{-1}).

Flight	Day	T_{bb}	Θ_{AIR}	R_N	$z_{i,m}$	H	U
16	210	300	292	-342	1500	239	4.7
17	211	295	290	-154	NA	88	3.4
19	215	302	292	-385	1600	289	2.0
2 6	222	290	287	-102	1300	69	4.9

Figures

1. Segment of digitized Landsat photograph in the region of 61^0N, -164.4 ^{0}W. Black stripe corresponds to one, 20 km flight segment during Flight 26.

2. Balloon soundings taken at the tower site, on the four flight days. Each day is represented by potential temperature profiles (left) and absolute humidity profiles (right). The number on the potential temperature graph is the Julian day, with the flight number in parentheses.

3. Plot of surface heat flux (Wm^{-2}) extrapolated from flight 16 flux profiles, against the mean radiative surface temperature (C) for each flight segment. Point marked "TOWER" represents the mean tower heat flux during the flight and the radiative temperature at the tower site derived from a downward-looking infrared radiometer. Points with error bars represent the means and standard deviations for each pattern flown during flight 16.

4. Typical heat flux profile from flight 16 with sources of uncertainty for flux estimates. The tower heat flux is marked on the lower axis.

5. Time series (at 5 Hz) of radiative surface temperature from PRT-5 (C) for a segment of flight 19.

6. A. Number histogram of lake "sizes", in consecutive 5 Hz points (1 point approximately 20 m), during a segment of flight 16.

B. Number histogram of observations of PRT-5 temperature values for the same segment as 4A.

7. Fraction of points classified as "lake" (represented by dots) as a function of longitude, derived from digitized Landsat image in Figure 1. Mean PRT-5 temperature (+) against longitude for 20 km segments of flight 26 flown in an east-west transect, with the linear regression line through these points.

8. Maximum mixed layer height (m) predicted in the "jump" model versus integrated daily heat flux recorded at the tower site. Actual z_i observations are denoted by triangles. The four flight days are also labelled. Horizontal lines represent the range of z_i observations observed by the DIAL instrument on flight 26.

9. A. Kinematic heat flux ($ms^{-1}K$) versus mean radiative surface temperature (C) from single-level flights 17(X), 19 (dots), and 26 (triangles). Corresponding values at the tower site are shown with symbols next to "T".

B. Kinematic moisture flux ($ms^{-1}gm^{-3}$) versus mean radiative surface temperature (C) from single-levle flights 17 (X), 19(+), and 26 (triangles).

10. A. Kinematic heat flux ($ms^{-1}K$) against the potential temperature of air minus the radiative surface temperature. Solid line represents the model values from the linear combination of fluxes from land and water, as explained in the text.

B. Kinematic moisture flux ($ms^{-1}gm^{-3}$) against air-suface temperature difference, as in 10A.

Austin, L. B. , P. H. Schuepp, and R. L. Desjardins ,The feasibility of using airborne CO_2 flux measurements for the imaging of the rate of biomass production, Agric. For. Meteorol. 39: 13-23, 1987.

Avissar, R. and M. M. Verstraete, The representation of continental surface processes in atmospheric models, Rev. Geophys. 28 (1) : 35-52, 1990.

Browell, et al. in press.

Dickinson, R. E. and A. Henderson-Sellers, Modelling tropical deforestation: A study of GCM land-surface parametrizations, Q. J. R. Met. Soc. 114: 439-462,1988.

Gibbons, J. D. , Nonparametric methods for quantitative analysis (2nd edition). American Sciences Press, Columbus OH. 481 pp.,1985.

Harriss, R. C., S. C. Wofsy, D. S. Bartlett, M. C. Shipham, J. M. Hoell Jr., R. J. Bendura, J. W. Drewry, R. J. McNeal, R. L. Navarro, R. Gidge, and V. Rabine, The Arctic Boundary Layer Expedition (ABLE-3A): July-August 1988, J. Geophys. Res., in press.

Hechtel, L. M., C-H Moeng, and R. B. Stull, The effects of nonhomogeneous surface fluxes on the convective boundary layer: a case study using large-eddy simulation, J. Atmos. Sci. 47 (14): 1721-1741,1990.

Jacob, D. J., et al., Deposition of ozone to tundra. J. Geophys. Res.,(in press).

Lenshow, D. H., R. Pearson, Jr., and B. B. Stankov, Estimating the ozone budget in the boundary layer by use of aircraft measurements of ozone eddy flux and mean concentration, J. Geophys. Res. 86: 7291-7297, 1981 .

Lenschow, D. H. and B. B. Stankov, Length scales in the convective boundary layer, J. Atmos. Sci. 43 (12) :1198-1209, 1986.

Luvall, J. C. and H. R. Holbo, Thermal remote sensing methods in landscape ecology. pp 127-152*in* M. G. Turner and R. H. Gardner, eds. Quantitative Methods in Landscape Ecology. Springer-Verlag, N. Y, 1991.

MacPherson, J.J., H. H. Neumann, G. den Hartog, R.L. Desjardins, K. M. King, and P.H. Schuepp, Comparison of aircraft and tower measured fluxes from the Northern Wetlands Study, Eos spring supplement :85 (abstract).

Mason, P. J. , The formation of areally-averaged roughness lengths. Bound.-Layer Met. 114: 399-420,1988.

Matson, P. A., P. M. Vitousek, and D. S. Schimel, Regional extrapolation of trace gas flux based on soils and ecosystems. pp. 97-108 *in* M. O. Andreae and D. S. Schimel, eds. Exchange of Trace Gases between Terrestial Ecosystems and the Atmosphere. John Wiley and Sons, N. Y.,1989.

Matheron, G., Principles of geostatistics, Econ. Geol. 58:1246-1266,1963.

Noilhan, J. , P. Lacarrere, and P. Bougeault, An experiment with an advanced surface parameterization in a mesobeta-scale model. Part III: Comparison with the HAPEX-MOBILHY dataset, Mon. Wea. Rev. 119: 2393-2413, 1991.

Oliveira, A. P. ,Planetary boundary layer dynamics over the Amazon rain forest. Ph.D. Dissertation, State University of New York at Albany, Albany, N. Y.,1990.

Ritter, J. A., J. D. W. Barrick, G. W. Sachse, G. L. Gregory, M. A. Woerner, C. E. Watson, G. F. Hill, and J. E. Collins, Airborne flux measurements of trace species in an arctic boundary layer. J. Geophys. Res, (in press).

Ritter, J. A., D. H. Lenschow, J. D. W. Barrick, G. L. Gregory, G. W. Sachse, G. F. Hill, and M. A. Woerner, Airborne flux measurements and budget estimates of trace species over the Amazon basin during the GTE/ABLE-2B expedition, J. Geophys. Res. 95 (D10): 16,875-16,886,1990.

Said, F. and A. Druilhet, Experimental study of the atmospheric marine boundary layer from in-situ aircraft measurements (TOSCANE-T campaign): variability of boundary conditions and eddy flux parameterization. Boundary-Layer Met. 57: 219-249, 1991.

Stewart, J. W. B. et al., 1989. Extrapolation of flux measurements to regional and global scales. in: M. O. Andreae and D. S. Schimel, eds. Exchange of Trace Gases between Terrestrial Ecosystems and the Atmosphere. J. Wiley and Sons. 347 pp.

Tennekes, H., A model for the dynamics of the inversion above a convective boundary layer, J. Atmos. Sci. 30: 558-567,1973.

Vihma, T. and H. Savijarvi, On the effective roughness length for heterogeneous terrain, Quart. J. Royal. Met. Soc. 117: 399-407, 1991.

Weil, J. C. and T. W. Horst, Footprint estimates for atmospheric flux measurements in the convective boundary layer.(in press)

Wetzel, P. J. and J-T. Chang, Evapotranspiration from nonuniform surfaces: a first approach for short-term numerical weather prediction, Mon. Wea. Rev. 116: 600-621, 1988.

Whiting, G. J., and D. S. Bartlett, CO_2 exchange in tundra environments and potential for remote sensing. Eos 70: 284 (abstract).

Wyngaard, J. C., Lectures on the planetary boundary layer, in Mesoscale Meteorology--Theories, Observations and Models, edited by D. K. Lilly and T. Gal-Chen, D. Reidel, Hingham, MA, 1983.

Yanai, M., S. Esbensen, and J.-H. Chu, Determination of bulk properties of tropical cloud clusters from large-scale heat and moisture budgets, J. Atmos. Sci. 30: 611-627, 1973.

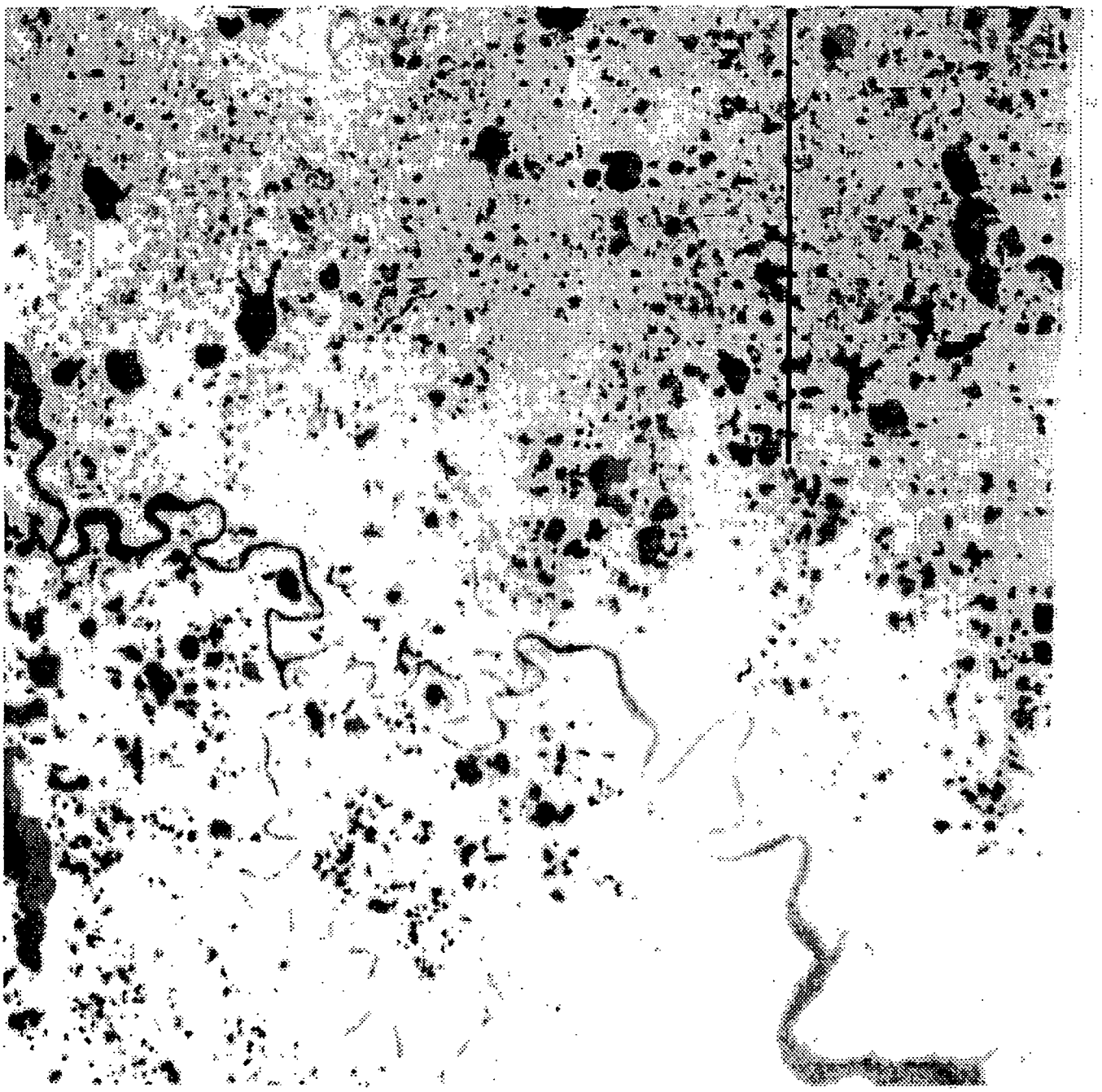

FIG-1

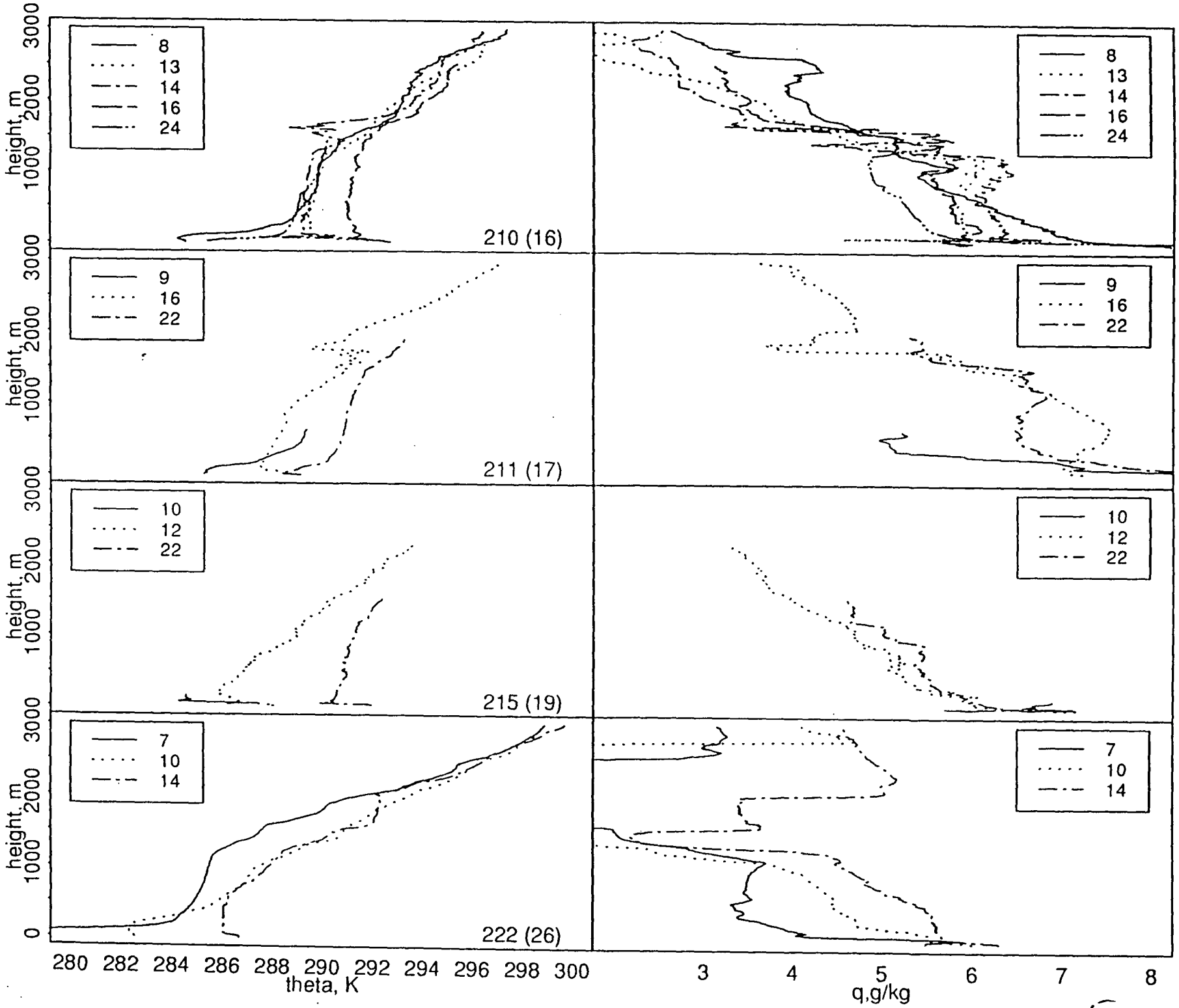
height, m
0
1000
2000
3000
8
13
14
16
24
210 (16)
9
16
22
211 (17)
10
12
22
215 (19)
7
10
14
222 (26)
280 282 284 286 288 290 292 294 296 298 300
theta, K
3 4 5 6 7 8
q,g/kg

FIG. 2

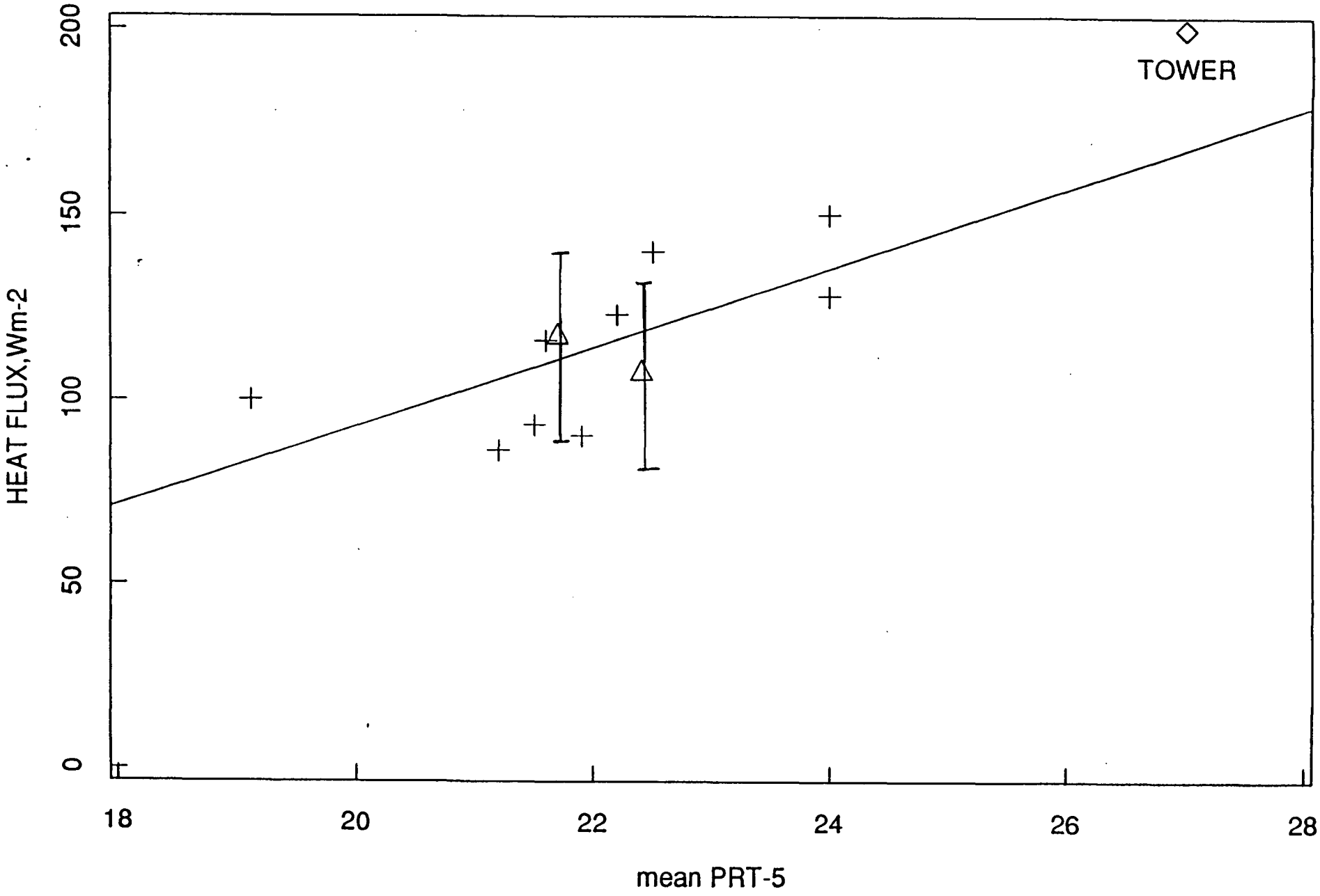

FIG. 3

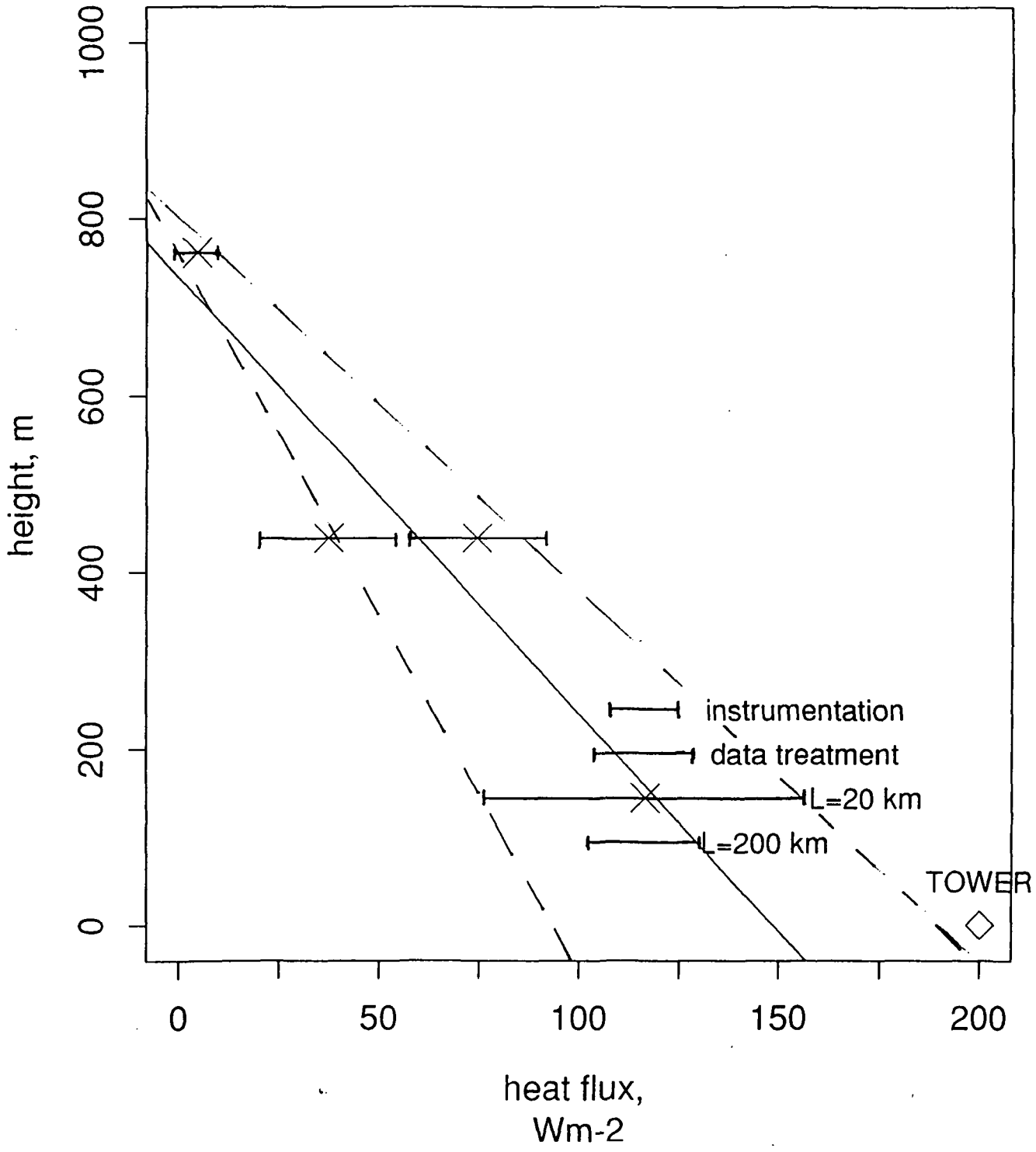
height, m
1000
800
600
400
200
0
0
50
100
150
200
heat flux,
Wm-2
instrumentation
data treatment
L=20 km
L=200 km
TOWER

FG.4

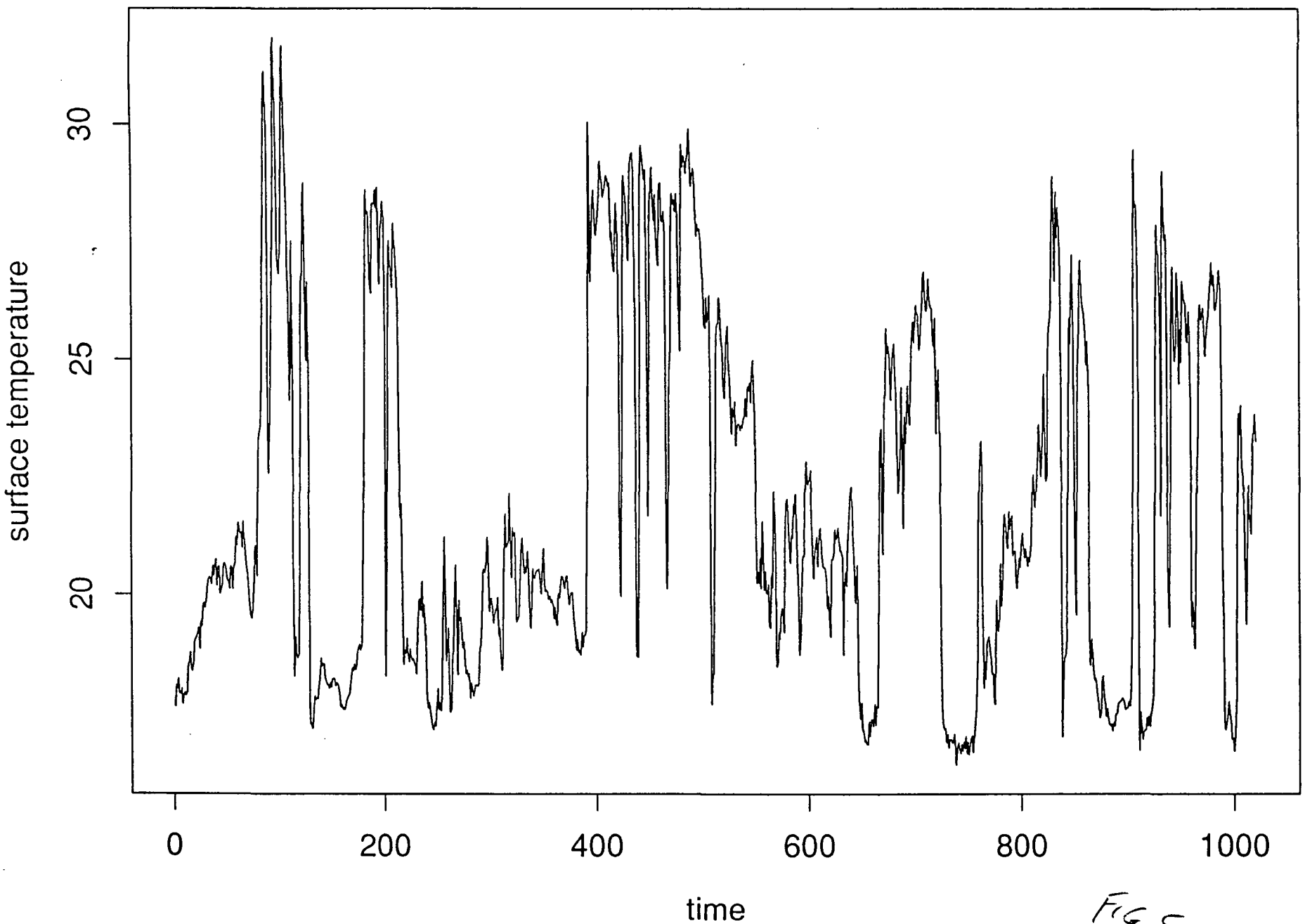

FIG. 5

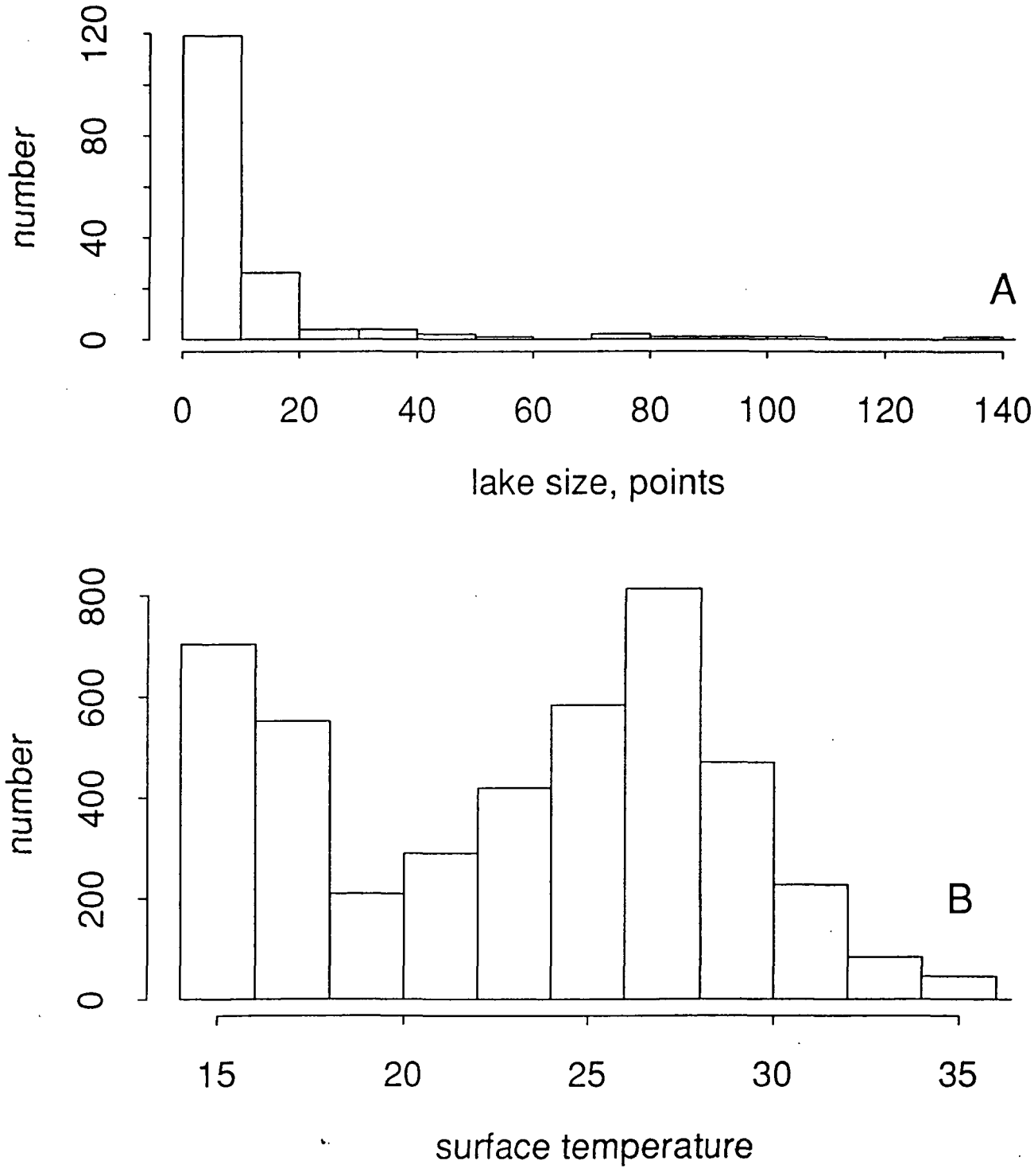
number
0
40
80
120
A
0
20
40
60
80
100
120
140
lake size, points
number
0
200
400
600
800
B
15
20
25
30
35
surface temperature

Fig. 6

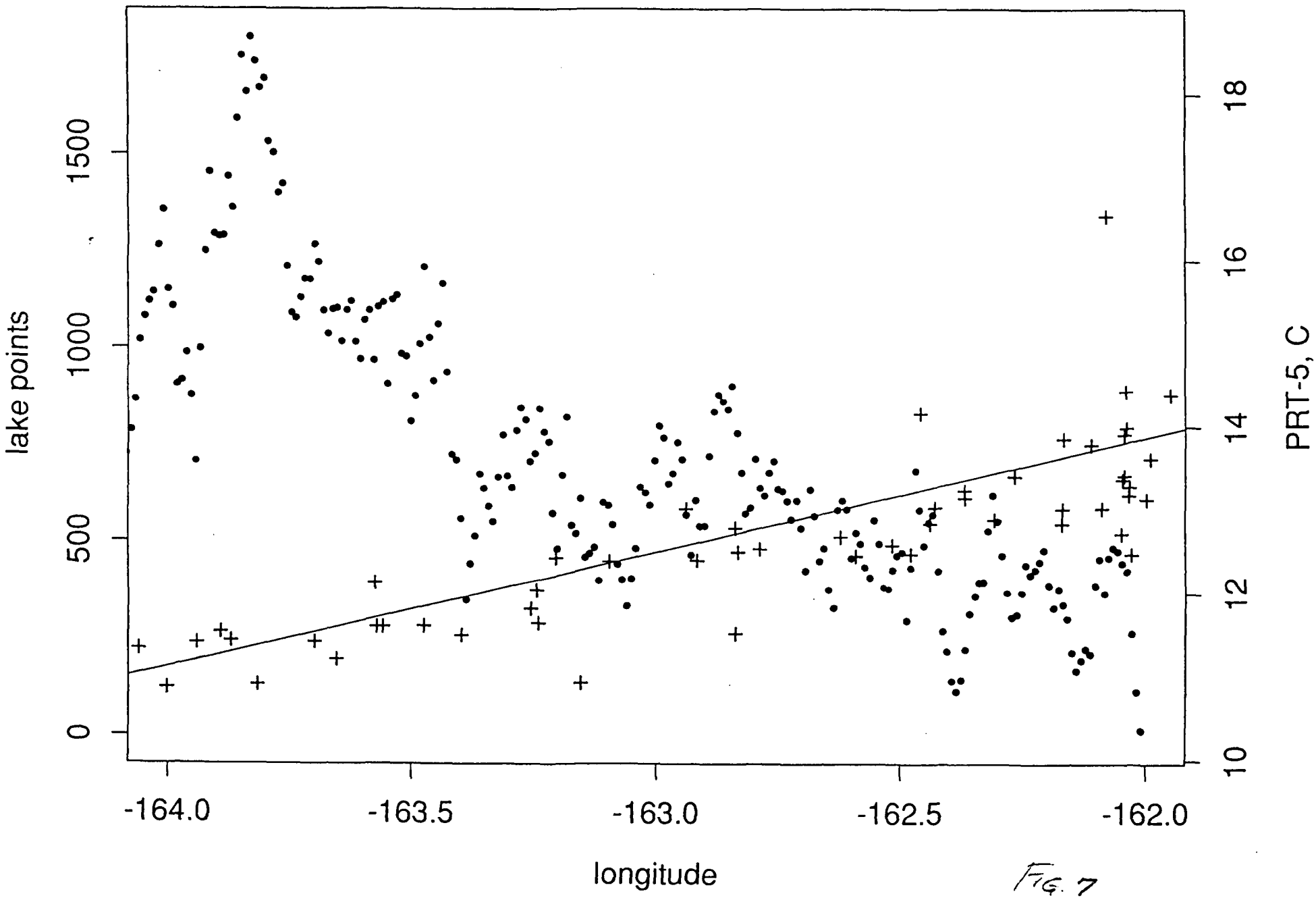
lake points
0
500
1000
1500
-164.0
-163.5
-163.0
-162.5
-162.0
longitude
PRT-5, C
10
12
14
16
18

FIG. 7

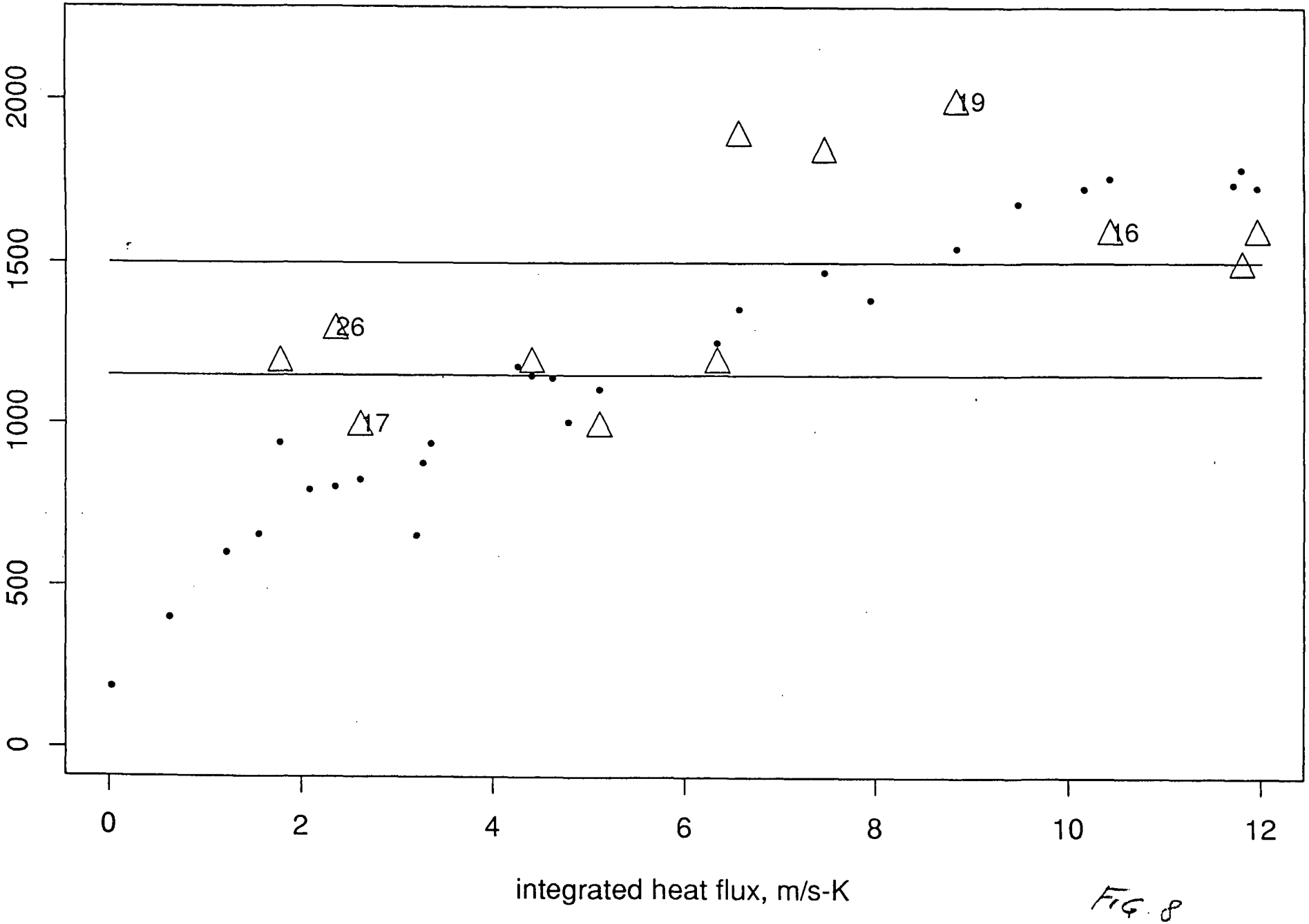
0
500
1000
1500
2000
0
2
4
6
8
10
12
integrated heat flux, m/s-K
19
16
26
17

FIG. 8

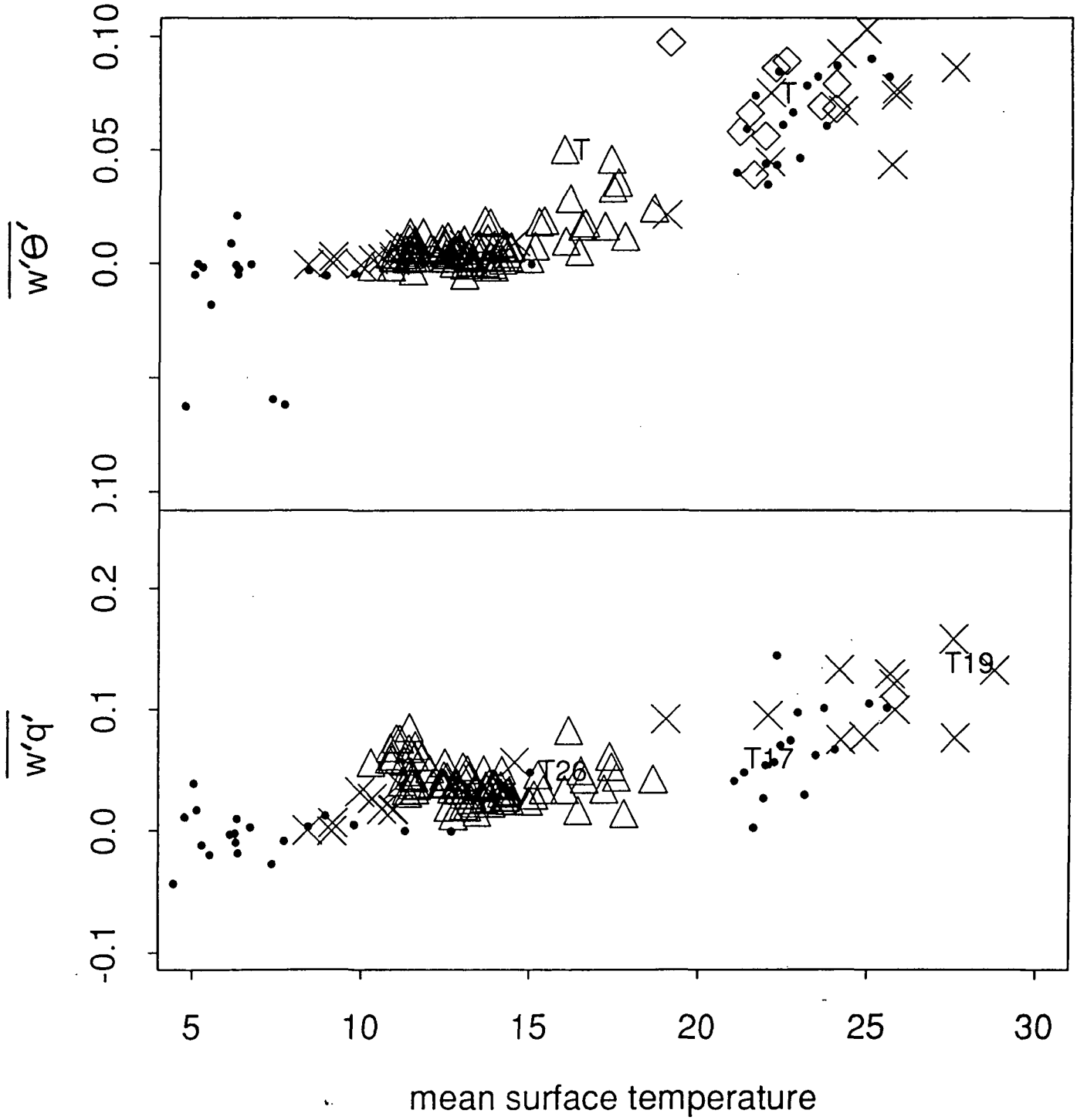
$\overline{w'\theta'}$
0.10
0.05
0.0
.10
T
T
$\overline{w'q'}$
0.2
0.1
0.0
-0.1
T19
T17
T20
5
10
15
20
25
30
mean surface temperature

FIG. 9

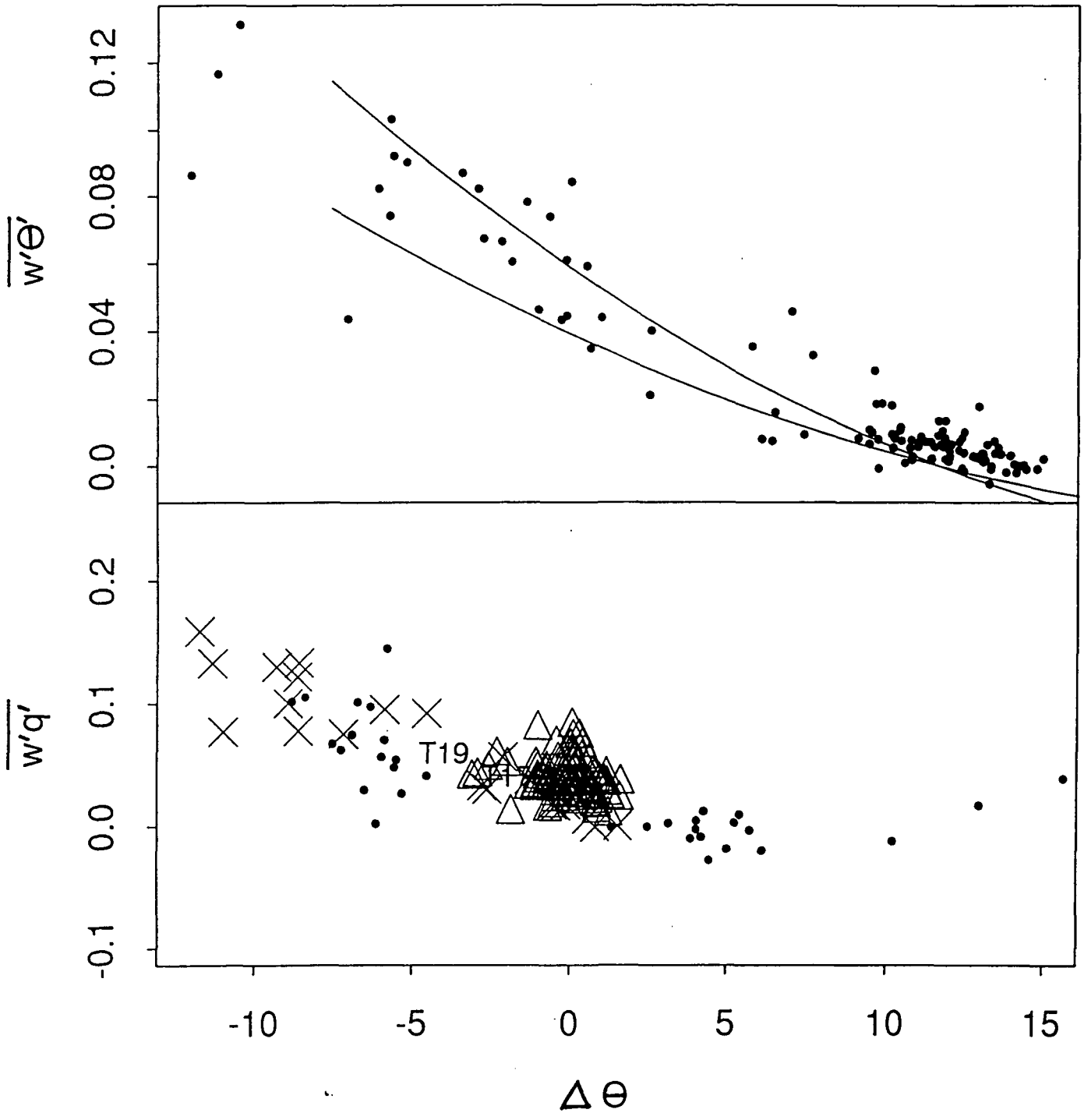
$\overline{w'\theta'}$
0.12
0.08
0.04
0.0
$\overline{w'q'}$
0.2
0.1
0.0
-0.1
T19
-10
-5
0
5
10
15
$\Delta\theta$

FIG. 10